C146-E178

SHIMADZU
Excellence in Science

GCxGC Handbook

Application Compendium of Comprehensive 2D GC Vol.1-5

Application of Comprehensive 2D GC Vol. 1 - 5

Prof. Luigi Mondello Università degli Studi di Messina

1. Analysis of Fresh and Aged Tea Tree Essential Oil

1.1 INTRODUCTION

Tea tree oil (TTO) is obtained through hydrodistillation of the aerial parts drawn from *Melaleuca alternifolia* L., a plant belonging to the family of *Myrtaceae* and commonly found in Australia. This product is widely employed in the cosmetic and pharmaceutical industry, and finds a privileged place in the market of herbal formulations and traditional remedies against a series of infections. Characteristic for this oil is its high sensitivity to oxygen and light exposure, which causes the transformation of specific constituents (mainly monoterpenes and their oxygenated derivatives) into oxidation products, responsible for important allergic phenomena. In particular, the literature reports a decrease of α-terpinene, γ-terpinene and terpinolene, with a simultaneous increase of *p*-cymene, ascaridole and 1,2,4-trihydroxymenthane.

In the application here presented, tea tree oil, which is definitely a complex sample from a chromatographic point of view, has been investigated by means of a GC×GC-MS system. The objective was not only to unravel the chemical composition of the essential oil, but more specifically to compare a fresh sample, retrieved from the market, with a very old one (about 25 years old). The methodology utilized was capable of detecting oxidation products, also where the latter were not expected, highlighting the high sensitivity of the method used. It must be noted that the wide consumption of tea tree oil and the harmful properties of oxidized products has led the Scientific Committee on Consumer Products to deliver an opinion on TTO in 2008 [1].

1.2 EXPERIMENTAL

1.2.1 Samples and sample preparation procedures

Fresh samples of TTO, produced by *Thursday Plantations* (Ballina, Australia), were purchased from a supermarket in Hobart (Tasmania, Australia). The oxidized TTO sample was kindly provided by *Essential Oils and Tea Tree Research Department of Wollongbar Primary Industries Institute* (Wollongbar, Australia).

All the TTO samples were diluted in ethanol (1:10, v/v) prior to injection into the GC×GC-MS system.

1.2.2 Configuration of the instrument

GC×GC-MS analyses were carried out on a Shimadzu *GC×GCMS-QP2010 Ultra* system. The GC was equipped with a split/splitless injector, an SLB-5ms (Supelco) column (30 m × 0.25 mm ID × 0.25 µm film thickness).

The primary column was connected to the secondary column (Supelcowax-10, 1 m × 0.1 mm ID × 0.1 µm film thickness) by means of a SilTite (SGE, Australia) mini-union. The modulator was a dual-stage loop-type one (Zoex, Houston, TX). The software packages utilized for data handling were *GCMSsolution* (Shimadzu) and *Chromsquare* (Shimadzu Europe, Germany).

Monodimensional GC-MS analyses were carried out exploiting the same GC×GC-MS system, connecting the SLB-5ms column directly to the MS detector.

1.2.3 Method parameters

GC oven program was from 50°C to 280°C at 3°C/min. Injection temperature was 280°C. Sample volume was 1.0 µL, injected in the split mode (1:100). Carrier gas (He) was delivered at an initial pressure of 133.3 kPa (constant linear velocity mode). The cryogenic modulation period was 6 s, and the hot pulse (325°C) duration was 375 ms.

Mass spectrometric parameters were as follows: scan speed of 10,000 amu/s, mass range of 40-400 *m/z*, sampling frequency of 20 spectra/s, detector voltage of 1.0 kV. Interface and ion source temperatures: 280°C and 250°C, respectively. MS ionization mode: electron ionization; detector voltage: 1.0 kV.

Monodimensional GC-MS analyses were performed with the following oven program: from 50°C to 280°C at 3°C/min. Sample volume was 1.0 µL, injected in the split mode (1:50). Carrier gas (He) was delivered at an initial pressure of 37.1 kPa (constant linear velocity mode: 32.4 cm/s). MS parameters as above reported except for scan speed (1,666 amu/s) and sampling frequency (4 spectra/s).

1.3 RESULTS AND DISCUSSION

The GC×GC-MS method developed allowed the simultaneous separation and identification of about 130 compounds in the samples of TTO analyzed, which are listed in Table 2.1 and visualized in Figures 2.1 to 2.4. One of the most relevant findings was the detection of 1,2,4-trihydroxymenthane and 2-methylisoborneol after running the samples in the comprehensive GC system, otherwise not detected due to their co-elution with viridiflorene. The latter (peak 104) was predominant compared to the other two constituents, and it was identified with a very good similarity score in the monodimensional GC-MS analysis (96%). Such an outcome would mean that the analyst would completely ignore the presence of the oxidation products, 1,2,4-trihydroxymenthane

and 2-methylisoborneol, if limiting his/her investigation to a monodimensional GC-MS analysis of TTO. The presence of the co-eluting compounds was also confirmed by comparing their 2D retention times with those obtained in the correspondent 2D chromatogram of the aged TTO (see Figure 2.5). It must also be emphasized that the limit of detection (LOD) changed consistently when passing from the GC-qMS to the GC×GC-MS method, which was another reason for the non-determination of 1,2,4-trihydroxymenthane in the monodimensional analysis.

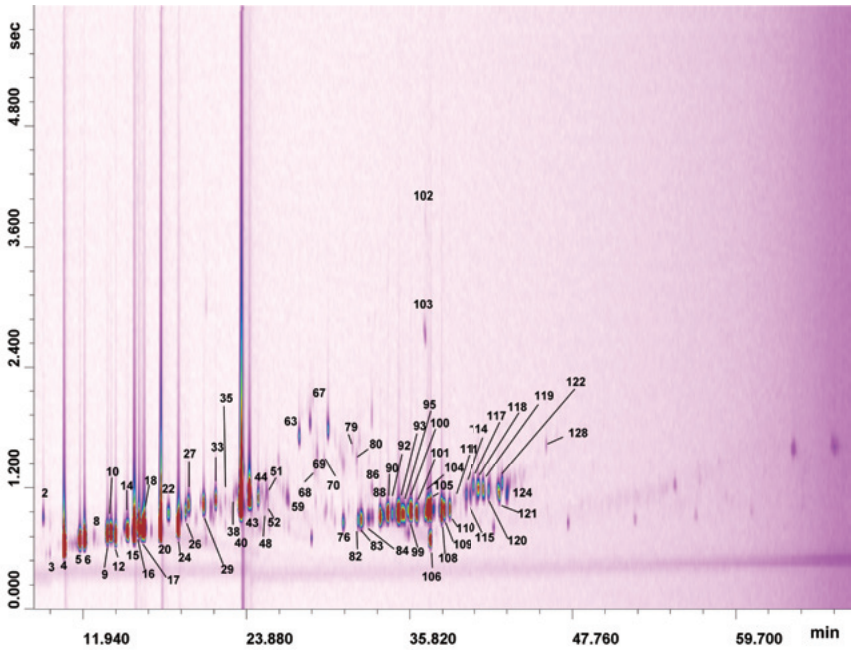

Figure 2.1

GC×GC-qMS chromatogram of fresh tea tree oil (see Table 2.1 for peak assignment).

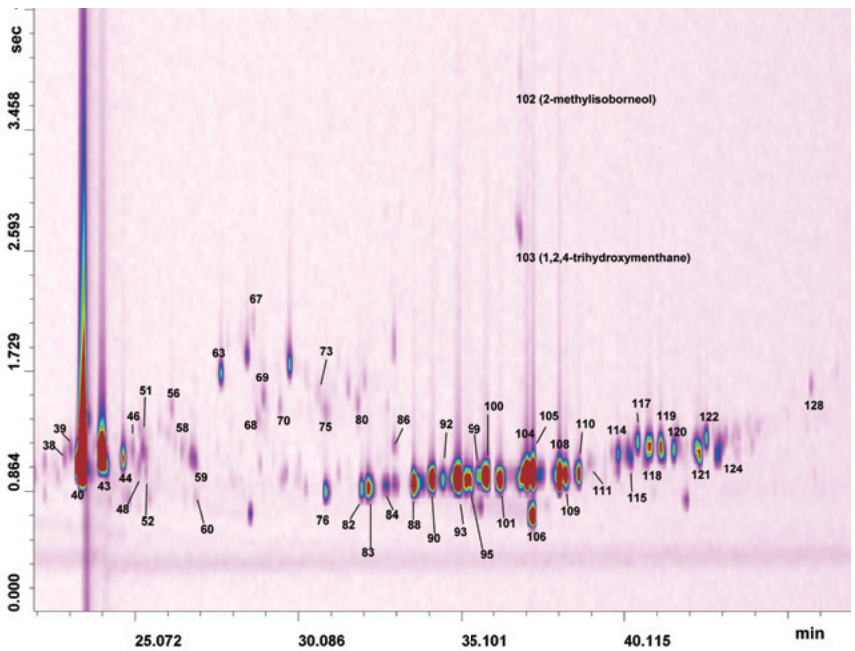

Figure 2.2

GC×GC-qMS chromatogram expansion of fresh tea tree oil (see Table 2.1 for peak assignment).

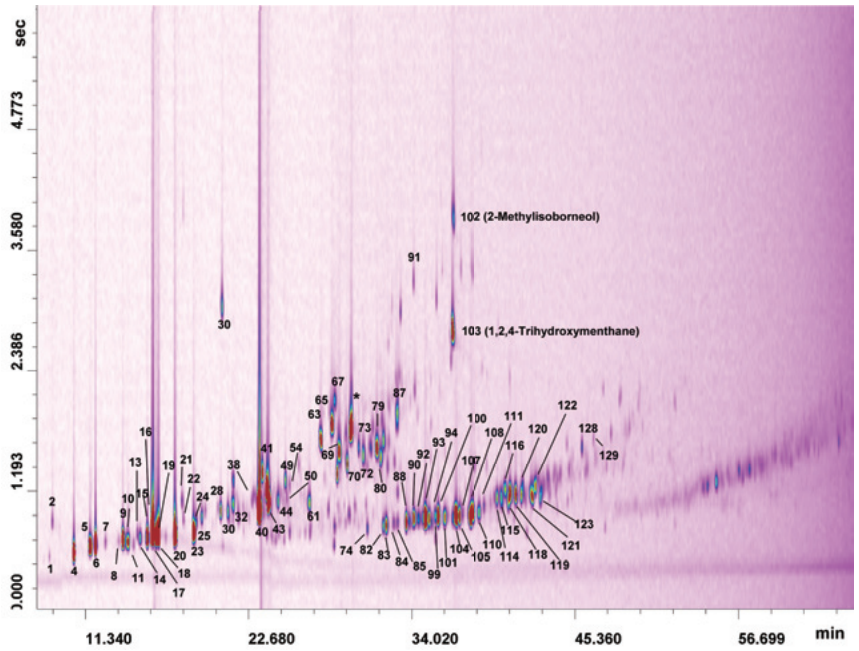

Figure 2.3

GC×GC-qMS chromatogram of aged tea tree oil (see Table 2.1 for peak assignment).

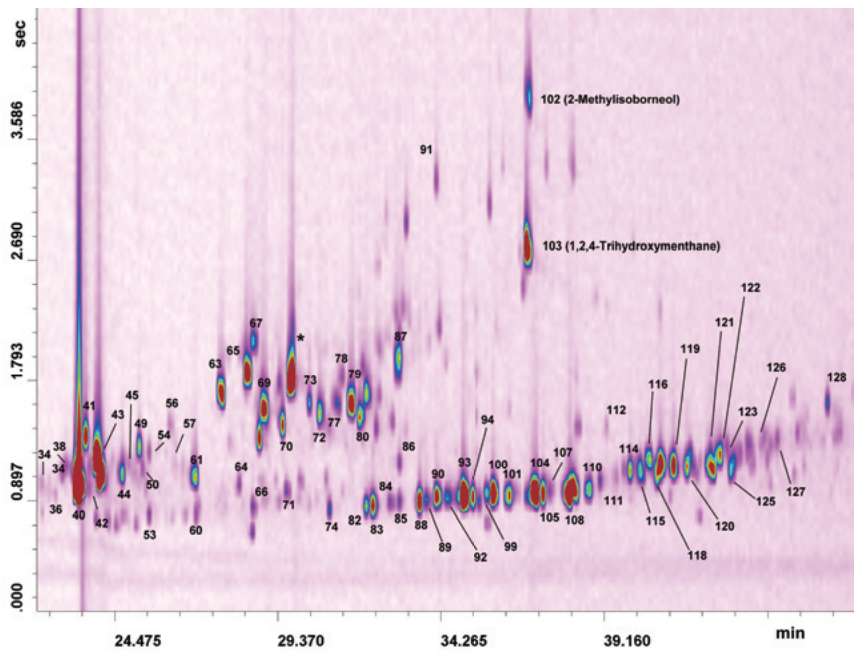

Figure 2.4

GC×GC-qMS chromatogram expansion of aged tea tree oil (see Table 2.1 for peak assignment).

Table 2.1

Compounds identified in the fresh (TTO1) and aged (TTO2) tea tree oil samples. Abbreviations: MS% = spectral similarity (values reported in parenthesis are GC-qMS results).

Peak No.	Compound	MS% TTO1	MS% TTO2
1	6-methyl-3,5-heptadien-2-one	-	86
2	*cis*-3-hexen-1-ol	98 (94)	96 (95)
3	3-methyloctane	94	-
4	nonane	85	98 (89)
5	α-thujene	98 (99)	96 (99)
6	α-pinene	95 (97)	97 (98)
7	camphene	90 (97)	94 (97)
8	sabinene	97 (97)	91 (98)
9	β-pinene	96 (97)	97 (97)
10	myrcene	98 (97)	97 (96)
11	2,3,6-trimethyl-1,5-heptadiene	-	93
12	2-undecene	81	-
13	*cis*-3-hexenyl acetate	98 (93)	96 (91)
14	α-phellandrene	98 (97)	97 (97)
15	α-terpinene	92 (96)	97 (97)
16	*p*-cymene	94 (98)	94 (81)
17	limonene	98 (95)	98 (97)
18	1,8-cineole	97 (92)	98 (92)
19	*trans*-β-ocimene	95 (98)	92 (96)
20	γ-terpinene	94 (89)	96 (95)
21	1,2-diacetylethane	-	88
22	*trans*-sabinene hydrate	93 (93)	92 (94)
23	terpinolene	96 (96)	98 (96)
24	*p*-cymenene	96 (95)	82 (81)
25	linalool	98 (98)	98 (97)
26	*cis*-sabinene hydrate	92 (96)	90 (94)
27	verbenene	81	-
28	fenchyl alcohol	95 (97)	90 (97)
29	*cis*-*p*-menth-2-ene-1-ol	95 (98)	96 (98)
30	1-terpineol	92 (96)	95 (98)
31	1,3-cyclohexadiene	90	-
32	*trans*-*p*-menth-2-ene-1-ol	96 (95)	90 (94)
33	*cis*-limonene oxide	84 (83)	81
34	camphene hydrate	92 (95)	81 (81)
35	*cis*-pinene hydrate	80	80
36	carvone oxide	-	80
37	*cis*-8-hydroxylinalool	83	-
38	γ-terpineol	93 (94)	95 (93)
39	borneol	89 (89)	-
40	terpinene-4-ol	90 (91)	94 (97)
41	*p*-cymen-8-ol	-	96 (94)
42	cryptone	-	86
43	α-terpineol	96 (97)	98 (97)
44	*trans*-piperitol	95 (92)	94 (94)
45	dehydrosesquicineole	-	80
46	1-p-Menthene-9-al	83	-
47	3,6-dimethyl- 1,5-heptadiene	-	87
48	santene	83	-
49	4,6-dimethyl-2-octanone	80	83
50	dehydrolinalool	-	85
51	*trans*-geraniol	85 (90)	-
52	isoascaridole	88 (88)	-
53	3-methyl-3-cyclohexen-1-ol	-	83
54	6-methyl-5-hepten-2-one	-	86
55	limonene epoxide	84	80
56	ascaridole epoxide	90	92
57	β-sanatlol	81	80
58	nerol	90(86)	-
59	piperitone	88(92)	-
60	apo vertenex	80	-
61	carvenone	-	93 (95)
62	*trans,trans*-2,4-dodecadienal	-	85
63	*trans*-ascaridole glycol	90 (91)	91 (91)
64	5-hydroxy-isobornyl isobutanoate	-	82
65	*cis*-ascaridole glycol	-	90
66	iso-thujyl acetate	-	85
67	carvacrol	85 (86)	96
68	2,5-dimethyl-2,4-hexadiene	81	-
69	1,3-dioxolane, 2,2-dimethyl-4,5-di-1-propenyl-	84	85
70	*cis*-linalool oxide	82	83
71	laciniata furanone E	-	80
72	*p*-menth-6-en-2,3-diol	-	82
73	*cis*-piperitol	80 (81)	82
74	β-cubebene	-	94 (98)
75	diepoxide allocimene	84	-
76	α-cubebene	94 (98)	-
77	menthone	-	80
78	dihydro-linalool acetate	-	82
79	4-methyl-dec-3-en-5-ol	80	82
80	1,4-cineole	80	83
81	α-methylenedodecanal	-	80
82	isoledene	93 (99)	93 (98)
83	α-copaene	94 (94)	94 (93)
84	β-elemene	95 (94)	93 (96)
85	longicyclene	-	87
86	methyl eugenol	94 (88)	92
87	isocaucalol	-	81

Peak No.	Compound	MS% TTO1	MS% TTO2
88	α-gurjunene	96 (96)	96 (96)
89	γ-maaliene	-	91 (90)
90	β-caryophillene	97 (97)	97 (97)
91	carvone hydrate	-	82
92	aromadendrene	93 (92)	92 (97)
93	9-epi-(E)-caryophyllene	91 (98)	91 (97)
94	selina-5,11-diene	-	90 (92)
95	germacrene D	90 (91)	-
96	hydroxy citronellal	-	80
97	6,7-epoxide citral	-	81
98	valerena-4,7(11)-diene	-	91 (89)
99	α-humulene	96 (97)	96 (96)
100	allo-aromadendrene	97 (90)	97 (96)
101	γ-gurjunene	87	93 (87)
102	2-methylisoborneol	77	85
103	1,2,4-trihydroxymenthane	90	93 (93)
104	viridiflorene	97 (96)	97 (94)
105	bicyclogermacrene	96 (97)	92 (89)
106	bicycloelemene	95	-
107	β-vetispirene	-	84
108	γ-cadinene	95 (94)	97 (91)
109	zonarene	93 (91)	-
110	*trans*-cadina-1(2),4-diene	97 (95)	92 (95)
111	α-calacorene	92 (97)	96 (99)
112	1(2H)-naphthalenone, 5-ethyl-3,4-dihydro-	-	80
113	caryophyllene oxide	-	80
114	viridiflorol	93 (93)	92 (95)
115	palustrol	92	90
116	ledol	-	90 (91)
117	isospathulenol	95 (96)	-
118	globulol	96 (92)	96 (93)
119	pogostol	86	88
120	rosifoliol	83	84 (83)
121	1-epi-cubenol	95 (97)	86 (85)
122	spathulenol	90	93
123	bicyclo[7.2.0]undecan-3-ol <11,11-dimethyl-,4,8-bis(methylene)->	-	86
124	cubenol	94 (97)	-
125	torreyol	-	92
126	hydroxycaryophyllene	-	90
127	cedrol	-	80 (82)
128	8-α-acetoxyelemol	83	82
129	flourensadiol	-	80

Another point of discussion is related to the determination of methyl eugenol (peak 86), which is a minor constituent of TTO but still regulated by the SCCP opinion. Specifically, this compound must be reported on the label due to its suspected carcinogenic nature. In the investigation here presented, GC×GC-MS demonstrated to be of great help even in this sense, due to a consistent improvement of the peak signal intensity which raised the similarity score from 88% to 94%. Sensitivity enhancement can greatly support the quantification of methyl eugenol, due to the analyte enrichment enabled through cryogenic modulation.

In general, the comparison between fresh and aged samples of TTO showed a similar qualitative profile but consistent quantitative differences: as expected, α-terpinene, γ-terpinene and terpinolene were lower in the aged sample, whereas *p*-cymene was approximately doubled. Other differences between the two profiles could be attributed to the higher amount of some components in the aged TTO: terpinen-4-ol, 1.5 times higher; 1,2,4-trihydroxymenthane, 18 times higher.

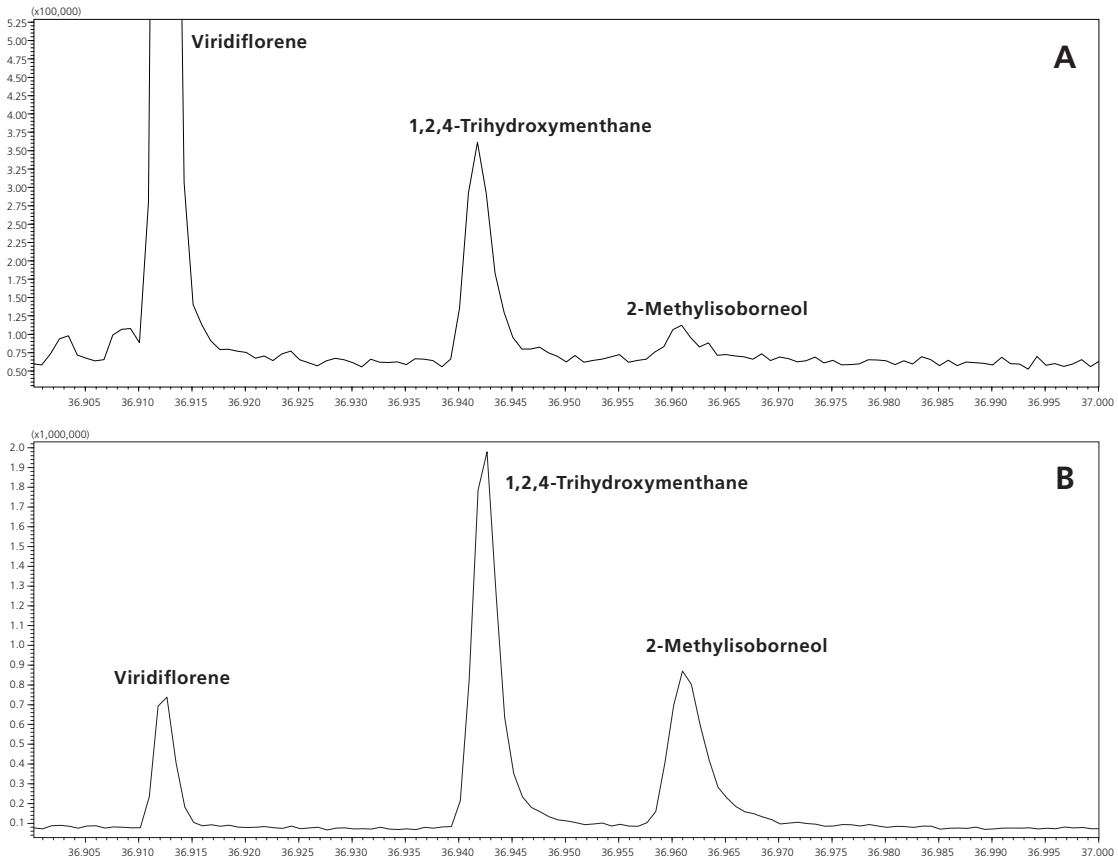

Figure 2.5

2D separation of 1,2,4-trihydroxymenthane in the fresh tea tree oil (A) and 2D separation in the aged tea tree oil (B).

1.4 CONCLUSION

The GC×GC-MS method demonstrated higher effectiveness and sensitivity compared to the monodimensional GC-qMS method in the investigation on tea tree oil. In fact, it allowed i) to determine a number of contact allergens not detectable with conventional methodologies; ii) to improve the method LOD, leading to the determination of trace compounds; iii) to give a reference for establishing the age of TTO (information on shelf-life).

Several compounds, although separated, couldn't be identified, very likely because not present in the mass spectral databases utilized.

2. Analysis of Perfume Allergens by Using Comprehensive 2D GC and a Rapid-Scanning Quadrupole Mass Spectrometer

2.1 INTRODUCTION

As stated in previous sections, separations occurring in the second dimension are really fast (generally 4-8 s), therefore making the use of very fast detectors necessary. Modulated peaks are typically 100-600 ms wide at the baseline. The history of GC×GC detectors was initially dominated by the FID; however, the necessity of structural information led to the use of MS instruments also in comprehensive GC. Quadrupole MS systems were then quite slow, and therefore more attention was devoted to the faster TOF-MS instruments; for example, the latter were utilized in 83% of the published work in the 2006-2009 period. However, this doesn't imply a lack of capability of quadrupole systems for GC×GC separations or the absolute predominance and excellence of ToF-MS systems over quadrupole MS. It must be specified that even ToF-MS instruments suffer from some limits: high data acquisition frequency instruments lack resolution, *viceversa*, high mass accuracy instruments lack acquisition speed. Furthermore, before the introduction into the market of very fast scanning qMS instrumentation (today available), some successful alternative attempts have been made, such as using a restricted mass range (e.g. 50-245 *m/z*), enabling the generation of 33 spectra/s [2], or using the ECNI (electron-capture negative ionization, Perkin Elmer) mode with a 300 amu mass range [3]. Both cases can be considered as "rapid scanning" methods.

Recently, Shimadzu has introduced a fast-scanning qMS system (*GCMS-QP2010 Ultra*) capable of operating at a scan speed of 20,000 amu/s. This instrumentation has been evaluated by G. Purcaro *et al*. in 2010, in an application on perfume allergens [4]. The latter have become a matter of great concern in the last years, with the dramatic increase of cases of contact allergy due to the use of cosmetic products. Because of such an occurrence, the EU has issued a series of regulations, one in particular being the EU Directive 2003/15/EC that fixes specific limits for these substances in different types of cosmetic products [5]. In their investigation, G. Purcaro *et al*. exploited a particular column set, consisting of apolar and ionic liquid stationary phases. Ionic liquids (ILs) fall into a class of organic non-molecular solvents, generally consisting of an organic cation containing nitrogen or phosphorous (*e.g.* phosphonium) counterbalanced by an anion of either organic or non organic nature.

2.2 EXPERIMENTAL

2.2.1 Samples and sample preparation procedures

A commercial fragrance was purchased in Messina (Italy) and was injected neat, without any sample preparation. A solution of twenty-four allergens was supplied by Sigma-Aldrich (Milan, Italy), along with 1,4-dibromobenzene and 4,4'-dibromobiphenyl, used as internal standards. Six working solutions were prepared in methanol for calibration procedures.

2.2.2 Configuration of the instrument

GC×GC-qMS analyses were carried out on a Shimadzu *GC×GCMS-QP2010 Ultra* system. The GC was equipped with a split/splitless injector, an SLB-5ms column (30 m × 0.25 mm ID × 0.25 µm film thickness), which was connected through a 1.4 m × 0.25 mm ID uncoated capillary segment (double loop) to the custom-made secondary column SLB-IL59 (1.0 m × 0.1 mm ID × 0.08 µm film thickness), all provided by Supelco. A loop-type modulator was used (Zoex, Houston, TX). The software packages utilized for data handling were *GCMSsolution* (Shimadzu) and *ChromSquare* (Shimadzu Europe, Germany), while the mass spectral database utilized was the *FFNSC* (Shimadzu).

2.2.3 Method parameters

GC oven temperature program was from 50°C to 260°C at 5°C/min. Injection temperature was 250°C. Sample volume was 1.0 µL, injected in the split mode (1:10). Carrier gas (He) was delivered at an initial pressure of 140.0 kPa (constant linear velocity mode). Modulation period was 4.5 s and the hot pulse (325°C) duration was 375 ms.

Mass spectrometric parameters were as follows: full scan mode; scan speed of 20,000 amu/s; mass range of 40-330 *m/z*. Interface and ion source temperatures: 250°C and 200°C, respectively.

2.3 RESULTS AND DISCUSSION

Figure 2.6 shows the GC×GC-qMS chromatogram obtained for the commercial fragrance analyzed. Twelve allergens were determined, all of them reported on the label, therefore at concentrations higher than those prescribed by the EU regulations for such products. Table 2.2 reports the quantitative results obtained from the calibration curves together with method repeatability results.

The chromatographic conditions were tuned in order to obtain optimal conditions. An acquisition frequency of 50 Hz was obtained

without the need for a restricted mass range or use of the SIM operational mode: scan speed was 20,000 amu/s, interscan delay was no more than 5 ms and mass range was 40-330 m/z. Four compounds were chosen, and here reported in Table 2.3, for assessing the extent of peak reconstruction. As can be seen from the data reported in Table 2.3, it is possible to have more than 10 data points/peak when operating at 25 Hz only if the peak width is above 400 ms, condition that increases the number of data points/peak to more than 20 when operating at 50 Hz. Additional information reported in the table is relative to the intensity ratio between the target ion (T) and the qualifier ions (Q1 and Q2). Figure 2.7 shows three plots, obtained at three different acquisition frequencies, relative to four parameters, namely the similarity match (MS%), the T/Q1 ratio, the T/Q2 ratio, the Q2/LM ratio (where LM is the lowest mass ion). The four peaks analyzed for their spectral quality showed constant MS% values at each data point and comparable T/Q ratios (limited peak skewing) under the different conditions investigated.

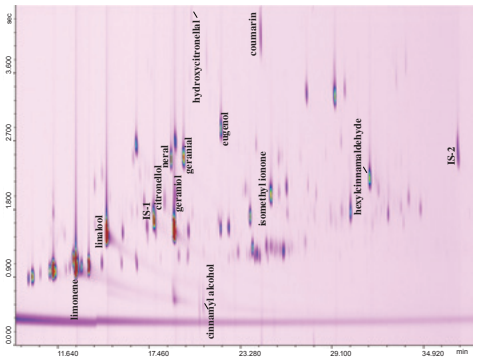

Figure 2.6

GC×GC-qMS chromatogram of a commercial fragrance. The compounds denominated are allergens. IS-1 and IS-2 are the internal standards. *Reprinted with permission from Anal. Chem., 2010, 82, 8583-8590. Copyright 2010 American Chemical Society.*

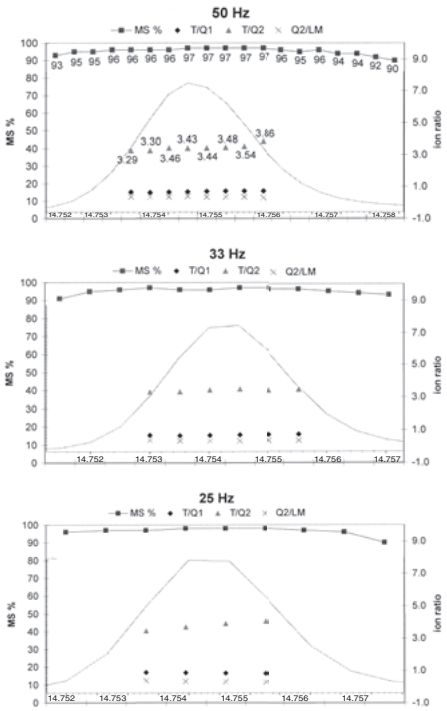

Figure 2.7

Spectral quality evaluation of linalool at 25, 33 and 50 Hz in terms of mass spectrum similarity (MS%) at each data point acquired and ion ratios across the width at half-height: T, 93 *m/z*; Q1, 71 *m/z*; Q2, 121 *m/z*; LM, 55 *m/z*. In the 50 Hz graph, MS and T/Q2 values at each data point acquired are shown. *Reprinted with permission from Anal. Chem., 2010, 82, 8583-8590. Copyright 2010 American Chemical Society.*

2.4 CONCLUSION

The present study has confirmed the validity of the novel quadrupole MS system for reliable quantification purposes in GC×GC. Satisfactory peak reconstruction was obtained with more than 15 data points/peak, demonstrating that the qMS system developed is a new and alternative option to the predominant use of ToF-MS instruments. It has been clearly demonstrated that even an acquisition frequency of 33 Hz can be sufficient for the achievement of proper peak reconstruction.

Table 2.2

Allergens identified and quantified in a commercial fragrance (n = 3)[a].

Reprinted with permission from Anal. Chem., 2010, 82, 8583-8590. Copyright 2010 American Chemical Society.

compd	concn (mg/L)	CV (%) (n = 3)	1D t_R (min)	SD	2D t_R (sec)	SD
limonene	4102.7	8.1	12.797	0.000	2.826	0.012
linalool	2721.1	5.3	14.755	0.001	3.288	0.047
citronellol	73.3	7.5	18.437	0.002	3.683	0.081
citral (neral)	455.1	3.0	18.895	0.001	4.232	0.065
geraniol	56.1	3.9	19.163	0.044	3.777	0.035
citral (geranial)	519.3	3.6	19.671	0.043	4.266	0.042
hydroxycitronellal	12.5	7.7	20.202	0.001	1.607	0.053
cinnamyl alcohol	54.8	11.4	20.889	0.002	2.304	0.071
eugenol	301.9	11.3	22.052	0.001	0.127	0.058
coumarin	187.9	1.7	24.622	0.001	1.319	0.046
isomethylionone	506.9	1.8	25.213	0.044	3.770	0.046
hexylcinnamaldehyde	462.1	2.3	31.492	0.001	3.984	0.042

[a] Retention times in the first and second dimensions (1D t_R and 2D t_R) are reported, along with the standard deviation (SD).

Table 2.3

Target Ion (T) and Qualifier Ions (Q1 and Q2) evaluated for each compound and Peak width at the baseline and at half-height and number of data points acquired for the main modulated peak of linalool, eugenol, lilial and benzyl salicylate.

Reprinted with permission from Anal. Chem., 2010, 82, 8583-8590. Copyright 2010 American Chemical Society.

					50 Hz				33 Hz				25 Hz			
compd	T	Q1	Q2	LM	peak width (ms)	no. of points	half-peak (ms)	no. of points	peak width (ms)	no. of points	half-peak (ms)	no. of points	peak width (ms)	no. of points	half-peak (ms)	no. of points
linalool	93	71	121	55	360	18	180	9	360	12	180	6	360	9	180	4
eugenol	164	103	149	55	480	24	240	12	480	16	240	8	480	12	240	6
lilial	189	147	204	57	420	21	190	10	420	14	180	6	360	9	180	5
benzyl salicylate	91	228	65		480	24	240	12	480	16	240	8	480	12	240	6

3. HS-SPME-GC×GC-MS Analysis of Yerba Mate (Ilex paraguariensis)

3.1 INTRODUCTION

Yerba mate is a beverage commonly consumed in South America. Its diffusion and composition remind xanthine-containing beverages, such as tea and coffee. Mate is obtained from the infusion of dried leaves and stems of a tree, *Ilex paraguariensis*; usually, the aerial parts of this plant are subjected to aging and/or roasting to improve the organoleptic properties. The plant has been studied for its biological properties, which have been reported to be many, such as hepatoprotective, neuro-stimulant, anti-rheumatic, ipocholesterolemic, and antioxidant. However, contamination with polycyclic aromatic hydrocarbons (PAHs) has also been found in this vegetable, therefore urging for a comprehensive and in-depth investigation on the volatile fraction.

In the present application, a GC×GC-MS method has been exploited, after an SPME step, for the analysis of yerba mate.

3.2 EXPERIMENTAL

3.2.1 Samples and sample preparation procedures

A mixture of hydrocarbons ranging from heptane to triacontane was provided by Supelco and was used for the measurement of retention indices.

A mate sample was purchased in a local market in Brazil (Rio Grande do Sul). The sample consisted of a 70:30 mixture of ground leaves and twigs of *I. paraguariensis*. For SPME extraction, about 150 mg of dried aerial parts were put in a 5 mL vial and subjected to extraction under the following conditions: DVB/Car/PDMS fiber (Supelco, USA), heating at 80°C for 15 min, shaking at 500 rpm, fiber exposure 60 min. Desorption of analytes occurred in the GC injector for 1.0 min at 250°C, in the splitless mode.

3.2.2 Configuration of the instrument

GC×GC-qMS analyses were carried out on a *GC×GCMS-QP2010 Ultra* system. Column set: first dimension, SLB-5ms (Supelco) column (30 m × 0.25 mm ID × 0.25 µm film thickness); second dimension: Equity 1701 (Supelco), 1.5 m × 0.10 mm ID × 0.10 µm film thickness. A dual-stage thermal modulator (ZOEX, Houston, USA) was used for analyte transfer from the first to the second dimension.

For bidimensional visualization, the *Chrom-Square* (Shimadzu Europe, Germany) software was used, while the mass spectral library utilized was the *FFNSC* (Shimadzu).

3.2.3 Method parameters

Oven temperature program was from 50°C (held 2 min) to 270°C at 3°C/min (held 15 min). Injection temperature was 280°C; injection mode: splitless, followed by a split ratio of 100:1. Carrier gas (He) was delivered at an initial pressure of 165.9 kPa (constant linear velocity mode). Modulation period was 6.0 s.

Mass spectrometric parameters were as follows: full scan mode, scan speed of 20,000 amu/s, mass range of 40-330 m/z, sampling frequency of 50 spectra/s. Interface and ion source temperatures: 250°C and 200°C, respectively.

3.3 RESULTS AND DISCUSSION

As can be seen in Figure 2.8, the sample was a highly complex one: over 1000 peaks were separated, 241 identified with a very good level of library matching (see Figure 2.9 and Table 2.4). The rapid scanning quadrupole, operated at 40-330 m/z mass range, produced 50 spectra/s, allowing for the acquisition of 14-16 data points per peak on average. Table 2.4 also reports linear retention index (LRI) data, that were calculated through the untransformed trace: considering each modulated fraction, in the case of an odd number of peaks, the retention time of the central one was taken into account; the retention time, in between the central couple, was taken into account in the case of an even number of peaks. Although the peak distribution in the chromatogram shown in Figure 2.8 appears random, group-type patterns can be traced as well: *e.g.*, the hydrocarbons that are distributed in the low part of the 2D space (non polar 2D zone). Depending upon the chemical nature of the groups separated, other bands of compounds can be visualized, such as carboxylic acids in the polar 2D zone, and aldehydes, ketones, alcohols in the medium-polarity zone.

Concerning the quantitative composition of the mate analyzed, caffeine, as expected, was determined as the predominant compound. However, many degradation products were present, which could be basically attributed to the heating process (drying or roasting). The latter, beyond enhancing the flavour notes with the production of furan derivatives (as in coffee flavour), also leads to carotenoid breakdown, proven by the presence of compounds such as 2,6,6-trimethylcyclohexanone, dihydroactinolide, beta-cyclocitral, and epoxy- derivatives. Also, many contamination products were detected, that are typically found in petroleum and mineral oil. Some polycyclic aromatic hydrocarbons (PAHs) were found, though

considering that such compounds are quite heavy, the HS-SPME process is not the most suitable technique in this case. Therefore, if a certain amount of PAHs were extracted from the present sample, it can be assumed that, with high probability, the original PAH content in the yerba mate was high. Many studies have previously demonstrated a conspicuous presence of PAHs in mate, sometimes comparable to a daily consumption of one packet of cigarettes per day [6].

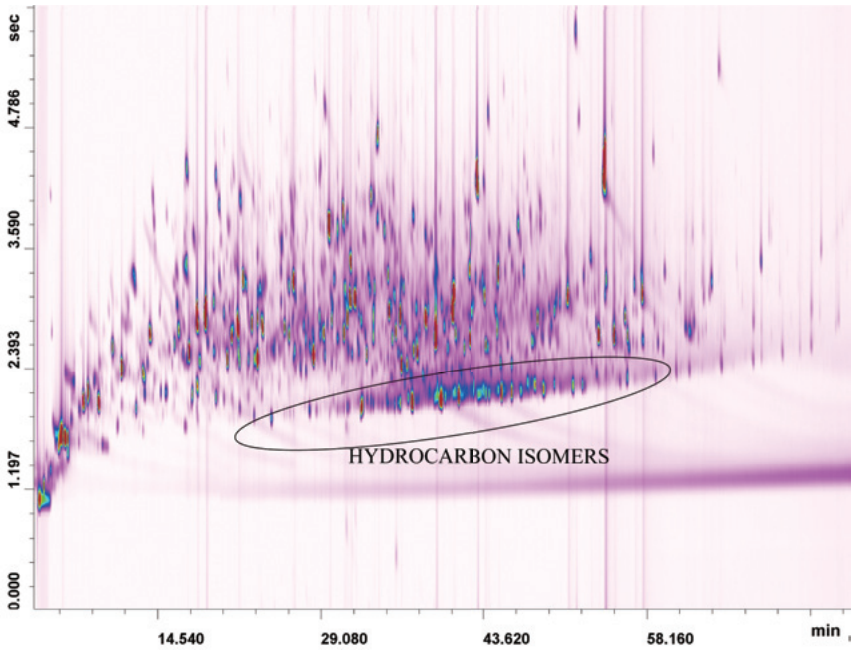

Figure 2.8

GC×GC-qMS chromatogram of a commercial sample of mate.

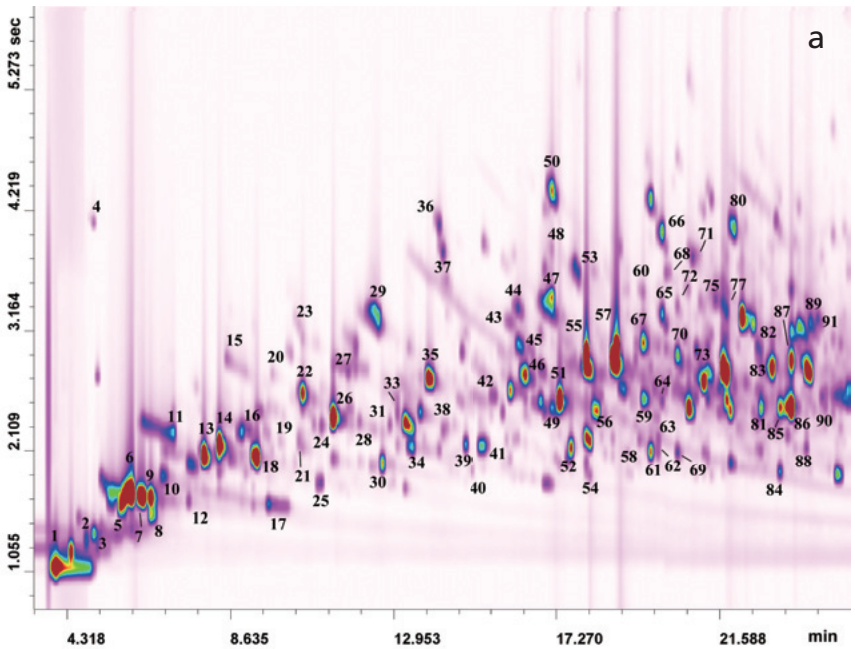

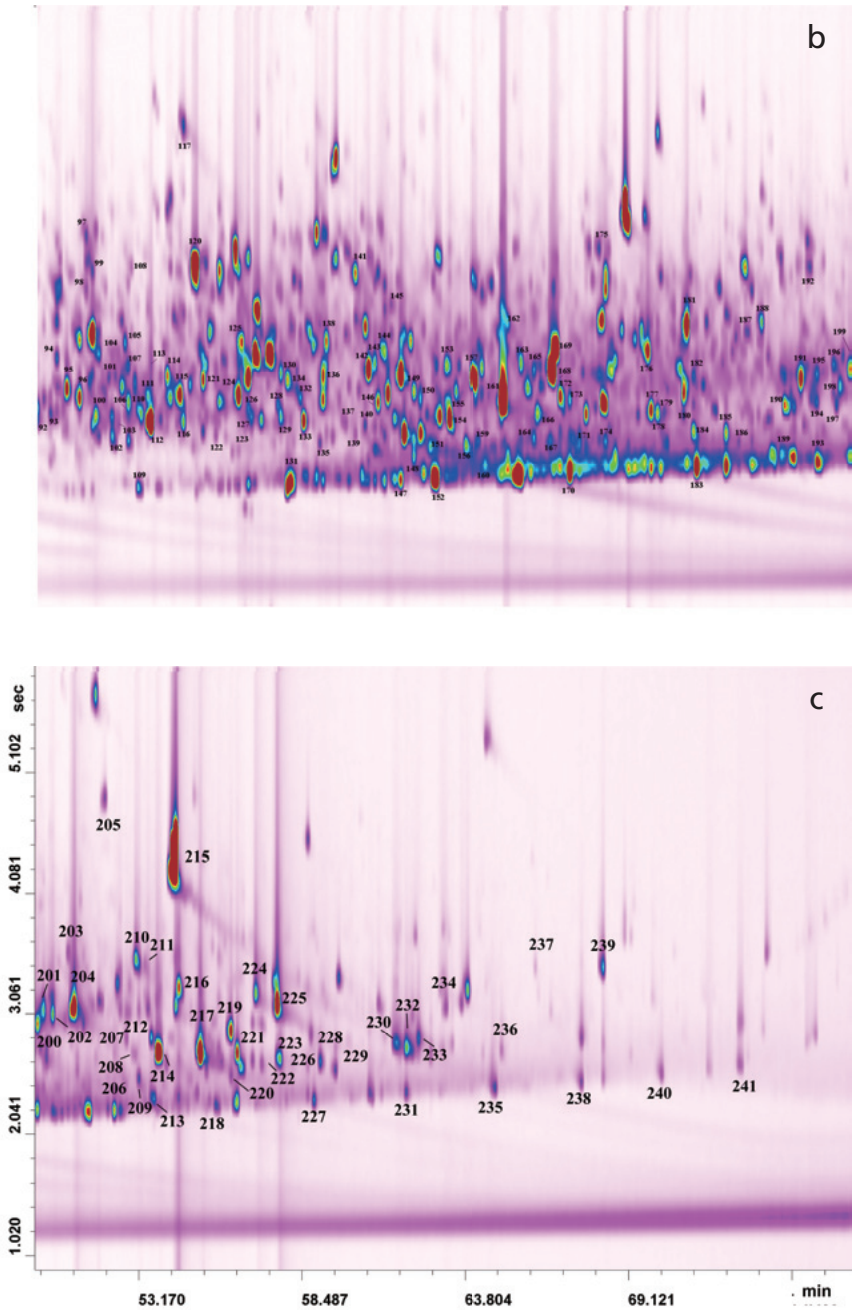

Figure 2.9

Three expansions (from *a* to *c*) of the chromatogram shown in Figure 2.8.

Table 2.4

Compounds identified in the mate GC×GC–qMS analysis; literature-derived (LRI_{lit}) and experimental LRI (LRI_{exp}) values and library match scores.

Peak No.	Compound	LRI_{lit}	LRI_{exp}	GCxGC-MS similarity%
1	propylene oxide	410		95
2	2-methylpropenal	574		90
3	2-methylbutyl acetate	590		90
4	ammonium acetate	630		99
5	2-butenal	615		98
6	acetic acid	576		99
7	1-penten-3-ol	680		96
8	2-ethyl furane	702	702	96
9	pentanal	704	702	96
10	acetol	698	713	94
11	propanoic acid	739	725	97
12	3-penten-2-one	733	739	96
13	2-pentenal	751	754	95
14	2-penten-1-ol,	767	769	96
15	butyric acid	773	777	97
16	3-methyl- 2-butenal	780	791	93
17	octane	800	800	98
18	hexanal	801	804	98
19	2-methyl-tetrahydrofuran-3-one	806	812	90
20	4-hydroxy-2-butanone	798	814	96
21	methylpyrazine	820	832	90
22	furfural	845	834	95
23	isovaleric acid	842	834	92
24	(2E)-hexenal	850	847	91
25	2-allylfuran	856	854	90
26	(2Z)-hexenal	850	854	98
27	furfuryl alcohol	860	864	96
28	hexanol	863	872	96
29	pentanoic acid	875	884	93
30	5-methyl-3-methylene-5-hexen-2-one	874	886	90
31	2-heptanone	898	892	98
32	nonane	900	901	98
33	4-heptenal,	902	901	97
34	2-butoxyethanol	936	910	97
35	2,4-hexadienal	914	914	95
36	2(5H)-furanone	924	920	98
37	gamma-butyrolactone	941	922	98
38	pyrazine, 2,5-dimethyl-	912	922	91
39	2,7-dimethyloxepine	954	934	91
40	alpha-pinene	932	938	95
41	2-octanone	952	955	94
42	2-heptenal,	956	959	97
43	2,2-dimethyl-3-heptanone	967	959	90
44	5-ethyl-2(5H)-furanone	968	963	91
45	5-methyl furfural	960	963	94
46	benzaldehyde	960	967	96
47	hexanoic acid	979	982	98
48	3-methyl-2(5H)-furanone	983	982	94
49	1-octen-3-ol	978	982	98
50	phenol	1011	982	97
51	6-methyl-5-hepten-2-one	986	986	98
52	2-pentyl-furan	991	992	95
53	3-hexenoic acid	983	995	96
54	decane	1000	1002	97
55	2,4-heptadienal steroisomer	1005	1000	96
56	octanal	1006	1006	97
57	(2E,4E)-heptadienal	1013	1016	97
58	para-cymene	1025	1028	94
59	2-ethyl-1-hexanol	1030	1030	98
60	2-cyclohexene-1,4-dione	1044	1031	92
61	limonene	1030	1034	97
62	beta-ocimene cis	1035	1038	90
63	1,8-cineole	1032	1038	94
64	2,2,6-trimethyl-cyclohexanone	1035	1040	93
65	benzyl alcohol	1040	1041	95
66	artemisia ketone	1042	1041	90
67	3-octen-2-one	1036	1042	93
68	gamma-, gamma-vinyl-valerolactone	1035	1043	94
69	trans-beta-ocimene	1046	1048	97
70	phenylacetaldehyde	1045	1048	96
71	2-methylphenol	1051	1057	98
72	2,5-dimethyl,4-hydroxy-3(2H)-furanone	1059	1061	91
73	2-octenal	1059	1062	97
74	gamma -terpinene	1058	1062	94
75	2-acetyl-pyrrole	1074	1069	90
76	(3E,5E)-octadien-2-one	1072*	1072	93
77	heptanoic acid	1073	1073	95
78	octanol	1063	1074	96
79	trans-linalool oxide	1073	1076	96
80	para-cresol	1071	1077	95
81	cis-linalool oxide	1087	1092	95
82	guaiacol	1087	1090	95
83	(3E,5Z)-octadien-2-one	1092*	1098	94

Peak No.	Compound	LRI_{lit}	LRI_{exp}	GCxGC-MS similarity%
84	undecane	1100	1100	97
85	linalool	1101	1102	96
86	nonanal	1104	1106	96
87	6-methyl-3,5-heptadien-2-one	1102	1108	96
88	4,8-dimethyl-1,3,7-nonatriene	1113	1116	93
89	maltol	1106	1118	90
90	2,4-octadienal	1113	1124	90
91	isophorone	1118	1130	91
92	non-3-en-2-one	1137	1142	90
93	trans-pinocarveol	1141	1150	90
94	oxophorone	1148	1150	95
95	(2E,6Z)-nonadienal	1153	1156	98
96	2-nonenal	1163	1164	95
97	benzoic acid	1150	1167	94
98	4-ethyl- phenol	1171	1169	94
99	3,5-dimethyl-phenol	1178	1173	93
100	1-nonanol	1155	1174	96
101	2,4-dimethyl-benzaldehyde	1190	1182	90
102	menthol	1184	1184	95
103	terpinen-4-ol	1180	1188	91
104	butyl diglycol	1211	1192	97
105	4,8-dimethyl-1,7-nonadien-4-ol	1182	1191	90
106	naphthalene	1178	1194	95
107	creosol	1190	1194	95
108	3,4-dimethyl-phenol	1191	1197	93
109	dodecane	1200	1200	99
110	alpha-terpineol	1195	1202	90
111	safranal	1201	1207	96
112	decanal	1208	1209	97
113	verbenone	1208	1218	90
114	2,4-nonadienal	1218	1220	93
115	beta.-cyclocitral	1217	1228	91
116	4,8-dimethyl-1-nonanol	1229	1230	90
117	hydroxy methyl furfural	1225	1231	93
118	3-methyl-3-(4-methyl-3-pentenyl)-2-oxiranecarbaldehyde	1215	1234	90
119	carvacryl methyl ether	1239	1243	91
120	3-ethyl-4-methyl-1H-pyrrole-2,5-dione	1238	1239	95
121	neral	1238	1243	95
122	linalyl acetate	1250	1251	95
123	geraniol	1249	1254	96
124	2-decenal	1265	1266	96

Peak No.	Compound	LRI_{lit}	LRI_{exp}	GCxGC-MS similarity%
125	nonanoic acid	1267	1269	94
126	geranial	1268	1273	95
127	decanol	1266	1275	96
128	(E)-anethole	1288	1292	96
129	2-undecanone	1293	1294	90
130	(2E,4Z)-decadienal	1292	1298	95
131	tridecane	1300	1300	94
132	2-methyl naphthalene	1308	1307	93
133	undecanal	1309	1309	97
134	4-vinyl-guaiacol	1309	1316	90
135	2-ethylhexyl butyrate	1317	1321	93
136	(2E,4E)-decadienal	1322	1323	97
137	4-tert-butylcyclohexyl acetate	1322	1339	94
138	triacetin	1346	1339	90
139	1,6-nonadien-3-ol, 3,7-dimethyl-, acetate	1344	1346	93
140	alpha-terpinyl acetate	1349	1353	93
141	2,6-dimethoxy-phenol	1347	1353	96
142	propanoic acid, 2-methyl-, 3-hydroxy-2,4,4-trimethylpentyl ester	1347	1355	91
143	eugenol	1357	1360	91
144	decanoic acid	1364	1366	96
145	gamma-nonalactone	1358	1367	96
146	8-undecenal	1365	1369	97
147	4-tertbutyl-cyclohexanol acetate	1368	1373	94
148	alpha-copaene	1375	1387	94
149	beta-damascenone	1383	1387	96
150	biphenyl	1380	1391	92
151	beta-elemene	1390	1398	93
152	tetradecane	1400	1400	97
153	vanillin	1394	1406	94
154	dodecanal	1410	1412	97
155	(E)-beta-damascone	1413	1417	90
156	longifolene	1412	1424	94
157	alpha-ionone	1421	1429	96
158	(E)-caryophyllene	1424	1434	96
159	dimethyl-naphthalene	1458	1439	93
160	cis-alpha-ambrinol	1439	1441	91
161	geranyl acetone	1455	1451	93
162	dimethyl-phthalate	1451	1454	91
163	acenaphthylene	1460	1466	91
164	allo-aromadendrene	1460	1475	90
165	7,8-epoxy-alpha-ionone	1473	1475	90
166	1-dodecanol	1469	1477	97

Peak No.	Compound	LRI_{lit}	LRI_{exp}	GCxGC-MS similarity%
167	germacrene D	1480	1487	91
168	(E)-beta-ionone	1490	1487	96
169	beta-ionone epoxide	1460	1492	95
170	pentadecane	1500	1501	98
171	alfa-muurolene	1496	1509	90
172	tridecanal	1516	1514	96
173	dihydro-apofarnesal	1516	1522	93
174	delta-cadinene	1518	1530	90
175	dihydroactinidiolide	1519*	1546	95
176	dodecanoic acid	1565	1563	96
177	(E)-nerolidol	1561	1566	97
178	hexa-hydro-farnesol	1563	1571	90
179	3-hexen-1-ol, benzoate	1573	1579	95
180	propanoic acid, 2-methyl-, 1-(1,1-dimethylethyl)-2-methyl-1,3-propanediyl ester	1605	1591	90
181	diethyl-phthalate	1592	1594	98
182	caryophyllene oxide	1587	1599	93
183	hexadecane	1600	1601	98
184	tetradecanal	1611	1615	95
185	isopropyl laurate	1615	1626	93
186	5-phenylundecane	1630	1637	92
187	benzophenone	1627	1645	92
188	triethyl-citrate	1659	1656	95
189	(E)-2-tetradecen-1-ol	1664	1672	91
190	tetradecanol	1671	1683	96
191	alpha-santalol	1676	1688	96
192	(2Z,6E)-farnesol	1679	1691	91
193	heptadecane	1700	1701	98
194	2-pentadecanone	1697	1702	94
195	(Z)-alpha-bergamotol	1690	1702	92
196	(2E, 6Z)-farnesal	1714	1716	90
197	pentadecanal	1702	1719	95
198	(Z,Z)-farnesol	1716	1722	97
199	(E)-beta-santalol	1738	1730	96
200	2,6-diisopropylnaphthalene	1727	1733	90
201	(Z)-nuciferol	1724	1736	91
202	(2E,6E)-farnesal	1737	1745	95
203	1H-phenalen-1-one	1751	1759	91
204	tetradecanoic acid	1769	1765	96
205	N-butyl- benzenesulfonamide	1797	1794	91
206	octadecane	1800	1802	97
207	2-ethylhexyl-salicylate	1805	1814	91
208	hexadecanal	1800	1820	94
209	isopropyl tetradecanoate	1826	1826	95
210	vetivenic acid	1812	1823	90
211	beta-vetivone	1821	1832	90

Peak No.	Compound	LRI_{lit}	LRI_{exp}	GCxGC-MS similarity%
212	5,9,13-trimethyl-4,8,12-tetradecatrienal	1855	1838	94
213	neophytadiene	1836	1840	92
214	phytone	1841	1847	96
215	caffeine	1841	1859	95
216	isobutyl phthalate	1908	1865	97
217	1-hexadecanol	1884	1885	97
218	nonadecane	1900	1900	98
219	farnesyl acetone	1913	1916	96
220	2-phenyltridecane	1922	1916	94
221	hexadecanoic acid, methyl ester	1925	1926	96
222	cyclohexadecanolide	1933	1942	90
223	isophytol	1947	1948	96
224	1-butyl 2-isobutyl phthalate	1973	1961	90
225	hexadecanoic acid	1977	1964	95
226	ethyl hexadecanoate	1993	1995	93
227	eicosane	2000	2002	98
228	hexadecyl acetate	2003	2009	96
229	isopropyl hexadecanoate	2023	2025	94
230	octadecyl acetate	2084	2092	96
231	heneicosane	2100	2102	97
232	methyl oleate	2085	2102	94
233	phytol	2106	2116	94
234	13-methyloxacyclotetradecane-2,11-dione	2137	2140	91
235	docosane	2200	2202	97
236	octadecanol acetate	2209	2209	91
237	tributyl-citrate acetate	2254	2250	91
238	tricosane	2300	2300	97
239	para-methoxy-, octyl-cinnamate	2321	2331	91
240	tetracosane	2400	2402	96
241	pentacosane	2500	2500	96

3.4 CONCLUSION

The GC×GC-qMS method developed in the present study allowed the detection of a high number of volatiles in yerba mate. The results have brought a more comprehensive knowledge on the chemical composition of a widely consumed product, especially with concerns to the presence of harmful constituents, such as PAHs and plasticizers. For such a reason, a future investigation could be devoted to a risk assessment study, considering the whole cycle of mate production (harvesting, treatment, marketing). Furthermore, and strictly from an analytical point of view, several components, whose identity remained unassigned in this study, could potentially be identified, maybe with the support of additional dedicated databases.

4. Comprehensive Two-Dimensional GC Analysis of Human Plasma Fatty Acids

4.1 INTRODUCTION

Dietary lipids are tightly related to a series of pathologies which have become very common in the modern society, such as hypertension, heart disease, diabetes, and hypercholesteremia. Public interest has been focused especially onto two particular classes of lipids, namely ω3 and ω6 polyunsaturated fatty acids, which have been demonstrated to act as artery cleaners.

In the present application, a highly sensitive GC×GC method for the determination of fatty acid methyl esters in human plasma is described. Methylation of the fatty acids was a necessary sample derivatization step, to improve the chromatographic separation (higher volatility, lower polarity). The method developed allowed to determine several fatty acids, some of them never reported before in human plasma.

4.2 EXPERIMENTAL

4.2.1 Samples and sample preparation procedures

Plasma samples were kindly supplied by a local clinic laboratory and analyzed as soon as received. The methylation procedure consisted of a saponification step, achieved by adding 1 mL of methanolic sodium methoxide to 100 µL of plasma, and held for 15 min at 100°C. After, the esterification was carried out through the addition of 1 mL boron trifluoride-methanol complex, again at 100°C for 15 min. FAMEs were then extracted by adding 1 mL of *n*-hexane to the mixture. A saturated NaCl solution was added to the mixture, agitated for 2 min and centrifuged. The last step consisted of sodium sulphate addition for water removal. The *n*-hexane layer was withdrawn, containing the FAMEs to be injected into the GC system.

4.2.2 Configuration of the instrument

GC×GC analyses were carried out on a Shimadzu *GC×GCMS-QP2010 Ultra* system. The GC was equipped with a split/splitless injector, an FID and the following column set: an SLB-5ms 30 m × 0.25 mm ID × 0.25 µm film thickness column was connected through a zero-dead volume press-fit to a Supelcowax-10 (0.95 m × 0.1 mm ID × 0.10 µm film thickness) capillary, both provided by Supelco. A loop-type modulator was used (Zoex, Houston, TX). The software packages utilized for data handling were *GCsolution* (Shimadzu) and *ChromSquare* (Shimadzu Europe, Germany).

4.2.3 Method parameters

Oven temperature program was from 180°C to 280°C at 3°C/min (held 10 min). Injection temperature was 280°C; injection mode: split, with a split ratio of 5:1. Carrier gas (H_2) was delivered at an initial pressure of 75.4 kPa (constant linear velocity mode). Modulation period was 6.0 s. FID gas flows: air, 400 mL/min; H_2, 40 mL/min, make-up (N_2), 40 mL/min. FID sampling rate: 8 ms.

4.3 RESULTS AND DISCUSSION

Dietary lipids have been extensively investigated by using chromatographic techniques in recent years. However, some drawbacks have arisen from conventional applications, consisting of: *i*) incapability of identifying the correct FA isomer in the case of double bond positional isomers, due to the high level of spectral similarity; *ii*) low separation power of the GC system; *iii*) trace level peaks not detected due to low sensitivity. The results obtained in the present study clearly showed that the GC×GC method developed allowed to overcome such problems. In fact, comprehensive GC is characterized by the following features: group-type distribution over the bidimensional space, which greatly helps peak identification (see point *i*); higher resolving power (see point *ii*); solute band reconcentration, that allows for trace peak detection (see point *iii*).

Figure 2.10 shows a GC×GC-FID chromatogram of a plasma sample (the most complex over a number of 10 samples analyzed). As can be seen, FAMEs distribute according to number of carbon atoms, number of double bonds, and position of double bonds. Such an ordered spatial distribution is highly useful for compound identity prediction. In fact, in this study 29 out of 65 peaks were identified on the basis of their location in the ordered contour plot (Table 2.5). As an example, Figure 2.11 shows an expansion relative to the bidimensional chromatogram shown in Figure 2.10 and reporting the C20 group. Peak 50 was assigned as $C_{20:4\omega3}$ since it is located at the intersection point between the DB4 (4 double bonds) band and the ω3 diagonal. This interpretation was further confirmed by the injection of the pure standard. Furthermore, peak 56 was tentatively identified as $C_{20:5\omega1}$ on the basis of its position, being unavailable the pure standard.

As previously mentioned, GC×GC succeeded in the determination of trace amount components, never reported before for human plasma. These were: odd-number saturated FAMEs such as $C_{11:0}$, $C_{19:0}$, $C_{21:0}$, and unsaturated ones, such as $C_{19:3}$, $C_{21:4}$, $C_{21:5}$.

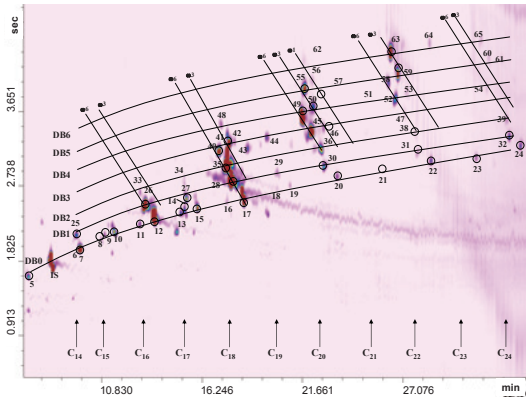

Figure 2.10

GC×GC-FID chromatogram of a human plasma FAMEs sample.

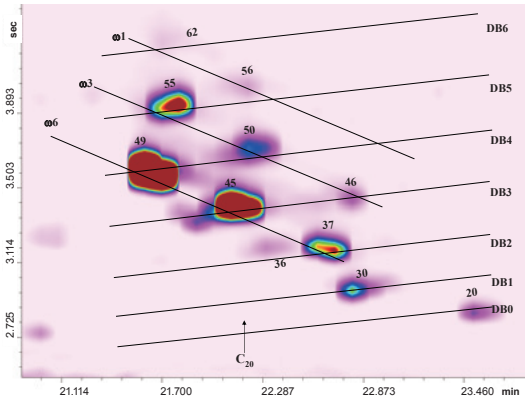

Figure 2.11

An expansion of the chromatogram shown in Figure 2.10.

Table 2.5

Identification of plasma FAMEs analyzed through GC×GC-FID.

Peak	FAME
1	C8:0
2	C9:0
3	C10:0 (st)
4	C11:0 (st)
5	C12:0 (st)
6	i-C14:0
7	C14:0 (st)
8	i-C15:0 (st)
9	a-C15:0 (st)
10	C15:0 (st)
11	i-C16:0 (st)
12	C16:0 (st)
13	i-C17:0 (st)
14	a-C17:0
15	C17:0 (st)
16	i-C18:0
17	C18:0 (st)
18	a-C19:0
19	C19:0
20	C20:0 (st)
21	C21:0 (st)
22	C22:0 (st)

Peak	FAME
23	C23:0 (st)
24	C24:0 (st)
25	C14:1ω5 (st)
26	C16:1ω7 (st)
27	C17:1ω7 (st)
28	C18:1ω9 (st)
29	C19:1
30	C20:1ω9 (st)
31	C22:1ω9 (st)
32	C24:1ω9 (st)
33	C16:2ω6
34	C17:2
35	C18:2ω6 (st)
36	C20:2
37	C20:2ω6 (st)
38	C22:2ω6 (st)
39	C24:2ω6
40	C18:3ω6 (st)
41	C18:3ω3 (st)
42	C18:3
43	C19:3
44	C19:3ω6

Peak	FAME
45	C20:3ω6 (st)
46	C20:3ω3 (st)
47	C22:3ω6
48	C18:4ω3
49	C20:4ω6 (st)
50	C20:4ω3 (st)
51	C21:4
52	C22:4ω6
53	C22:4ω3
54	C24:4ω6
55	C20:5ω3 (st)
56	C20:5ω1
57	C21:5
58	C22:5ω6
59	C22:5ω3 (st)
60	C24:5ω3
61	C24:5
62	C20:6ω1
63	C22:6ω3 (st)
64	C23:6
65	C24:6ω3

4.4 CONCLUSION

The study here presented has demonstrated the usefulness of GC×GC as a source of new information for a sample type that is characterized by relatively low complexity, but high scientific interest. Thanks to the highly ordered spatial distribution of analytes over the 2D plane, it was possible to assess the identity of almost 30 FAMEs. Indeed, it must be emphasized that of the compounds assigned, only a half has been identified by means of standard injection.

Also, a final remark should be given about the high sensitivity shown by the GC×GC method toward the determination of odd-numbered saturated and unsaturated fatty acids, at a very low concentration level (*ca*. 0.01%).

5. Analysis of Roasted Coffee Beans Aroma by Using Comprehensive Two-Dimensional GC Combined with Quadrupole Mass Spectrometry

5.1 INTRODUCTION

Coffee is today the most popular beverage in the world, with enormous implications in terms of economy and social life. Coffee cherries are obtained from two important plant species: *Coffea arabica* L. and *Coffea canephora* Pierre ex A. Froehner (syn. *robusta*). Coffee beans are typically produced in specific areas of the world, such as South America and North Africa. Coffee, as commonly consumed, is not a raw plant product, but it needs to undergo a roasting process for the development of its unique aroma. As a matter of fact, the "Arabica" species is considered as having a finer flavour compared to "Robusta". Usually, it is possible to find blends of the two types on the market, with a percentage composition depending upon the final character desired ("strong", "mild", "expresso", etc.). Several studies have reported the chemical composition of coffee aroma, highlighting variables such as the geographic origin, the species, the treatment, and so on. The aroma of roasted coffee is characterized by the presence of thousands of volatiles, mainly belonging to the chemical groups of furans, pyrazines, pyrroles, etc. Biosysnthetic routes of volatiles in coffee have been widely explored, and it seems reasonable that they derive from non volatile components contained in the green bean, which undergo breakdown and further reactions upon roasting. All these volatiles vary in olfactive power, concentration, chemical nature, and mutually interact to give coffee its unique taste.

As previously mentioned, coffee has been already extensively investigated. However, the high complexity of such a sample makes the list of its constituents far from complete. For this reason, comprehensive GC-MS has been exploited to investigate the volatile composition of commercial coffee beans, both from Arabica and Robusta species.

5.2 EXPERIMENTAL

5.2.1 Samples and sample preparation procedures

For each extraction, one halved coffee bean was put into a 2 mL headspace vial and subjected to solid phase microextraction process by means of a 50/30 µm fibre (divinylbenzene/carboxen/polydimethylsiloxane), purchased from Supelco. Samples were conditioned for 10 min at 60°C; after this period, the fiber was exposed to the headspace for 40 min at 60°C. After extraction was completed, analytes were desorbed into the GC injection

port for 1.0 min at 250°C. Blank runs were performed after two consecutive analyses.

5.2.2 Configuration of the instrument

GC×GC-qMS analyses were carried out on a Shimadzu *GCMS-QP2010 Ultra* equipped with a Zoex loop-type modulator. The column set was polar-apolar, being constituted of: 1D) Supelcowax-10 (30 m × 0.25 mm i.d. × 0.25µm d_f); 2D) SPB-5ms 1.0 m × 0.10 mm i.d. × 0.10 µm d_f. A loop-type modulator was used (Zoex, Houston, TX). The software packages utilized for data handling were *GCMSsolution* (Shimadzu) and *ChromSquare* (Shimadzu Europe, Germany), while the mass spectral database utilized was the *FFNSC* (Shimadzu). Comprehensive GC data handling was made by *ChromSquare* (Shimadzu Europe, Germany).

5.2.3 Method parameters

GC oven program temperature started from 60°C (held 5 min), raised up to 230°C at 1.5 °C/min, then to 280°C (held 2 min) at 50°C/ min. The modulation period was 5.0 s. Helium carrier gas was delivered at a constant pressure of 267.3 kPa, and the split/splitless injector (250°C) was held in splitless mode for 1.0 min, then operated in the split mode (70:1) for the rest of the analysis.

The temperature of the GC-MS interface was 250°C, and the detector voltage was 0.9 kV. A mass range of 40–330 was applied, and spectra were acquired at a rate of 50 Hz.

5.3 RESULTS AND DISCUSSION

Figure 2.12 shows a GC×GC-MS fingerprint of an Arabica coffee sample. As can be seen, the separation of analytes, carried out on a polar-apolar column set, provided a satisfactory result as previously reported in GC×GC-FID research carried out by Mondello *et al*. [7]. Furthermore, the figure highlights the high complexity of coffee flavour, with at least a thousand blobs spread out on the bidimensional plane. The rapid-scanning qMS instrument enabled the application of a normal mass range (40-330 amu) at a scanning rate of 50 spectra/sec, which was sufficient for both reliable peak identification and correct peak re-construction.

Also in this case, the "behaviour" of homologous analytes with respect to ordered spatial distribution can be noticed, as shown in Figure 2.13. Here, 14 pyrazines, aligned along distinct horizontal bands, depending upon the number of carbon atoms in the side chain, can be seen.

Although characteristic and high-quality

pyrazine mass spectra were generated, these were characterized by very similar fragmentation patterns. Peak identification was achieved by combining MS information, with that derived from the specific pyrazine location and one-dimensional LRIs. The amount of information derived from a GC-qMS application on the same sample was very far from that generated in the GC×GC-qMS experiment.

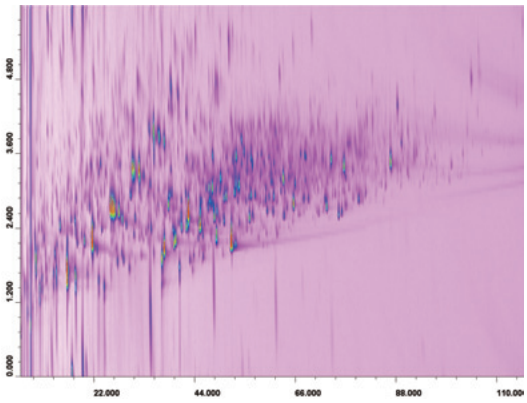

Figure 2.12
GC×GC-MS profile of the Arabica roasted coffee bean aroma.

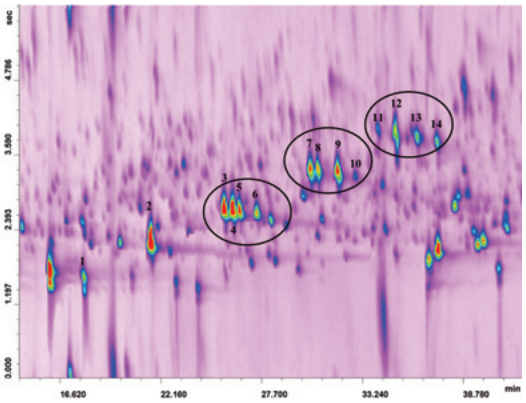

Figure 2.13
An expansion of the chromatogram reported in Figure 2.12, showing the pyrazine class. **1**: pyrazine; **2**: methylpyrazine; **3**: 2,5-dimethylpyrazine; **4**: 2,6-dimethylpyrazine; **5**: ethylpyrazine; **6**: 2,3-dimethylpyrazine; **7**: 2-ethyl-6-methylpyrazine; **8**: 2-ethyl-5-methylpyrazine; **9**: trimethylpyrazine; **10**: n-propylpyrazine; **11**: 2,6-diethylpyrazine; **12**: 2,5-dimethyl-3-ethylpyrazine; **13**: 2,6-dimethyl-3-ethylpyrazine; **14**: tetramethylpyrazine.

5.4 CONCLUSION

The high resolving power of comprehensive GC was applied to the study of a very complex sample, such as coffee aroma. The method developed allowed to reach the near to complete separation of all analytes present in the headspace of roasted coffee. A comprehensive knowledge of coffee aroma constituents can greatly help in assessing its quality.

References

[1] SCCP (Scientific Committee on Consumer Products), Opinion on tea tree oil, 16 December 2008.

[2] Adahchour, M.; Brandt, M.; Baier, H.-U.; Vreuls, R.J.J.; Batenburg, A.M.; Brinkman, U.A.Th. *J. Chromatogr. A*, **2005**, *1067*, 245-254.

[3] Korytár, P.; Parera, J.; Leonards, P.E.G.; de Boer, J.; Brinkman, U.A.Th. *J. Chromatogr. A*, **2005**, *1067*, 255-264.

[4] Purcaro, G.; Tranchida, P.Q.; Ragonese, C.; Conte, L.; Dugo, P.; Dugo, G.; Mondello, L. *Anal. Chem*. **2010**, *82*, 8583-8590.

[5] Directive 2003/15/EC of the European Parliament and of the Council of 27 February 2003.

[6] Kamangar, F.; Schantz, M.M.; Abnet, C.C.; Fagundes, R.B.; Dawsey, S.M. *Cancer Epidemiol. Biomarkers Prev*. **2008**, *17*, 1262-1268.

[7] Mondello, L.; Casilli, A.; Tranchida, P.Q.; Dugo, P.; Costa, R.; Festa, S.; Dugo, G. *J. Sep. Sci.*, **2004**, *27*, 442-450.

Shimadzu Corporation
www.shimadzu.com/an/

Printed in Japan 3655-07209-10AIT